

New triplet silylenes M–Si–M'–X along with some unusual cyclic forms (M = Li, Na, and K; M' = Be, Mg, and Ca; X = F, Cl, and Br)

Samaneh ASHENAGAR¹, Mohamad Zaman KASSAEE^{1,2,*}¹Department of Chemistry, Tarbiat Modares University, Tehran, Iran²Department of Chemical and Biomolecular Engineering, Vanderbilt University, Nashville, TN, USA

Received: 12.02.2018

Accepted/Published Online: 02.04.2018

Final Version: 03.08.2018

Abstract: Comparison of 54 M–Si–M'–X species is carried out using quantum mechanical ab initio and DFT computations at B3LYP/6-311++G**, QCISD(T)/6-311++G**, and CCSD(T)/6-311++G** levels of theory (M = Li, Na, K; M' = Be, Mg, Ca, and X = F, Cl, Br). All triplet species with M = K appear more linear than their corresponding ones with Li and Na. The electronegativity reactivity descriptor for each halogen (X = F, Cl, Br) is used as a tool to evaluate the interrelated properties of these silylenes. Stability, assumed as singlet–triplet energy difference (ΔE_{S-T}) for each series depends on the substituent's electropositivity, analyzed by applying appropriate isodesmic reactions. Stability of triplet M–Si–M'–X silylenes increases as functions of electropositivity of α -substituents and of β -substituents. The purpose of the present work was therefore to assess the influence of different di-alkaline metals with different β -substituents on the singlet–triplet energy gaps.

Key words: Triplet silylene, electropositivity, energy gaps, α and β substituent effects, multiplicity

1. Introduction

Sextet divalent silylenes have evolved from exotic reaction intermediates to important chemical species.¹ They have a low ability for hybridization, as their *s*-orbital is more constricted than the *p*-orbital.^{2–8} As the chemistry of triplet silylenes is expected to be entirely different from that of singlets, the preparation of a silylene that has a triplet ground state and the development of its chemistry is one of the most challenging concerns in the modern organo-silicon chemistry.^{9–14} Experimentally, generation of stable triplet silylenes is very difficult and has encountered many failures. In 1991, Gaspar succeeded in generating a triplet silylene with very large substituents.¹⁴ Theories have predicted that with electropositive Li substitution triplet ground-states will be more stable than the corresponding singlets.^{15–18} In 1985, Apeloig studied the influence of electropositive substituents at the divalent silicon atom and pointed out that these substituents stabilized its triplet state.⁹ Therefore, after disappointing attempts to isolate alkali-metal-substituted silyl radicals, in 2008, Sekiguchi et al. generated silyl radical (tBu₂MeSi)₂SiM structures (M = Li, Na, K) with the first group alkali-metals like Li, Na, and K.¹⁹ In fact, the more electropositive SiH₃, Li, Na, and K groups reduce the computed ΔE_{S-T} . The magnitude of the singlet–triplet splitting (ΔE_{S-T}) as well as the preparations of triplet states has received particular attention.^{10–12,20–23} The enormity of ΔE_{S-T} depends on the geometry of the molecule since the wider R-Si-R angle, the more stable the silylene triplet state.^{24–26} The development in this field in recent years

*Correspondence: mohamad.z.kassae@vanderbilt.edu

is principally impressive. Obviously, the rapid expansion of triplet silylene and germylene chemistry is evident due to their applications in electronics and other productions.^{27–29}

Some researchers have addressed interesting questions of how the presence of substituents affects the relative stabilities of triplet silylenes. We have already reported how electropositive substituents like Li, Na, and K affect the relative stabilities of different alkali-metal triplet germylenes.²⁹ Clearly, electronegative substituents increase the singlet–triplet energy gap, whereas electropositive substituents reduce the gap. In this paper we use density functional theory (DFT) computations to predict the effect of electronegative β -substituents along with electropositive α -substituents on the stability of triplet silylenes. The results show our theoretical investigation on singlet and triplet structures of 54 different di-alkaline metal silylenes with M–Si–M'–X formulation (M = Li, Na, K, M' = Be, Mg, Ca, and X = F, Cl, and Br) (Scheme 1).



Series 1; M = Li, M' = Be, Mg, Ca, X = F, Cl, Br

Series 2; M = Na, M' = Be, Mg, Ca, X = F, Cl, Br

Series 3; M = K, M' = Be, Mg, Ca, X = F, Cl, Br

Scheme 1. Schematic portrayal of a silylene in this study (Series 1–3).

2. Computational methods

All geometry optimizations are carried out without any symmetry constraints by means of hybrid functional B3LYP^{30–35} and the standardized 6-311++G** basis set, using the GAMESS package of programs.^{36,37} Both restricted and unrestricted B3LYP density functional methods for singlet states are available in the GAMESS, allowing the dynamics to be studied at different levels of accuracy with the DFT results expected to provide more accurate structural and energetic results. Moreover, triplet states are calculated with a spin-unrestricted wave function.³⁸ To obtain more accurate energetic data, single point computations are performed at the QCISD(T) and CCSD(T) levels of theory using the 6-311++G** basis set.³⁹ The S^2 expectation values of these species all showed a rather ideal value (2.001) after spin annihilation, so that their geometries are reliable for this study. The frequency calculations are applied to characterize the structures as minima (the number of imaginary frequencies (NIMAG = 0) or transition states (NIMAG = 1)).⁴⁰

3. Results and discussion

To achieve accessible triplet ground states of M–Si–M'–X species (M = Li, Na, K; M' = Be, Mg, Ca and (X = Li (1s,t), Table 1; X = Na (2s,t), Table 2; and X = K (3s,t), Table 3)), we compare thermodynamic and geometrical parameters for 54 new silylenic isomers at B3LYP/6-311++G**, CCSD(T)/6-311++G**, and QCISD(T)/6-311++G** levels of theory (Figure 1). Among our isomers, only two singlet structures (K–Si–Ca–Cl and K–Si–Ca–Br) undergo rearrangement upon optimization, forming rather long linkages from K to Ca (3.88 Å and 3.92 Å, respectively) and transform into cyclic structures (Figure 1). Clearly, for chlorine and bromine substituents at the silicon center, it is observed that in two cases the expected structures collapse to three-membered cyclic systems with the formation of weak bonds involving the calcium, potassium, and one of the bromine or chlorine atoms (Figure 1). This phenomenon is consistent with the convergence reported for

XGeCBr₃ and XGeCCl₃ molecules to unexpected structures, using the same DFT functionals (X = H, F, Cl, Br, and I).⁴¹

The structural parameters for the silicon compounds are collected (Figure 1). Clearly, in going from F → Cl → Br, variations of M–Si bond lengths in most of the structures are small, but M'–X bond lengths become longer as the atomic sizes of the halogen substituents increase (Br > Cl > F).

Furthermore, it is observed that the bond angles for all molecules in their singlet ground states lie in the range 80.0°–98.4°. The lone pair on the silicon atom causes a larger repulsion compared to the analogous repulsion of the bonding pair of electrons; hence the ideal angle of 120° is decreased significantly. This lone pair “occupies” a large space and consequently results in divalent angles less than 120°. Clearly, in all series the values of the divalent angles Si–M'–X increase as follows: F < Cl < Br. In Series 3, from the singlet to the triplet states, there is a decrease of nearly 0.2 Å in the M–Si bond lengths, while the expected increase in the bond angle is about 100°. Typically, there is an unexpected decrease in the M–Si–M' and Si–M'–X (M' = Be, Mg) bond angles of nearly 15° and 5° in Series 1 and 2. The magnitudes of the Si–Ca–X bond angle in nearly all triplets are more than those of their corresponding singlets. These structural changes may be related to the decreasing electron density around the divalent silicon center in the molecular plane from the singlet state to its corresponding triplet species. The halogen ligands linked to magnesium get closer to the silicon atom and achieve a better screening of the bonding electrons (Figure 1).

The other results obtained in the present research include DFT calculations and isodesmic reactions for 54 isomers of divalent silylenes. In addition, the zero point energies (ZPE) of these species are calculated for each optimized structure at B3LYP/6-311++G**. For the sake of brevity, selected harmonic frequencies of our species are included in the supplementary information.

With respect to substituents of these structures, the singlet–triplet energy gaps (ΔE_{S-T}) are employed to compare the relative stabilities at B3LYP/6-311++G**, QCISD(T)/6-311++G**, and CCSD(T)/6-311++G** levels of theory. The trends in the singlet–triplet energy gaps computed using the high-level QCISD(T) and CCSD(T) single-point energies are similar to that computed using the B3LYP-optimized energy (Tables 1–3).

B3LYP/6-311++G** as well as QCISD(T)/6-311++G** order of singlet–triplet energy gaps calculations between 1s–M'–X and 1t–M'–X show a trend of: $\Delta E_{S-T, Be-F}$ (–10.33 kcal/mol, –9.10 kcal/mol) > $\Delta E_{S-T, Be-Cl}$ (–2.93 kcal/mol, –3.98 kcal/mol) > $\Delta E_{S-T, Be-Br}$ (–2.91 kcal/mol, –3.85 kcal/mol) and $\Delta E_{S-T, Mg-F}$ (–3.48 kcal/mol, –5.59 kcal/mol) > $\Delta E_{S-T, Mg-Cl}$ (–3.35 kcal/mol, –5.42 kcal/mol) > $\Delta E_{S-T, Mg-Br}$ (–3.32 kcal/mol, –5.39 kcal/mol) and $\Delta E_{S-T, Ca-F}$ (–5.08 kcal/mol, –9.50 kcal/mol) > $\Delta E_{S-T, Ca-Cl}$ (–4.94 kcal/mol, –8.64 kcal/mol) > $\Delta E_{S-T, Ca-Br}$ (–4.94 kcal/mol, –8.30 kcal/mol) (Table 1). Apparently, the structures with the most electronegative β -substituent (X = F) have the lowest singlet–triplet energy gaps.

Clearly, the presence of a fluorine substituent destabilizes σ orbitals at M', meaning that triplets with fluorine substituents are more stable than triplets with chlorine and bromine substituents. Obviously, with reducing the electronegativity of β -halogens, stability of singlet state increases.

However, all the odds are in favor of existence of the triplet silylenes. The same levels of theory have been computed order of singlet–triplet energy gaps, $\Delta E_{S-T, M'-X}$, between 2s–M'–X and 2t–M'–X are: $\Delta E_{S-T, Be-F}$ (–7.33 kcal/mol, –8.26 kcal/mol) > $\Delta E_{S-T, Be-Cl}$ (–7.30 kcal/mol, –8.11 kcal/mol) > $\Delta E_{S-T, Be-Br}$ (–7.09 kcal/mol, –7.84 kcal/mol) and $\Delta E_{S-T, Mg-F}$ (–7.53 kcal/mol, –8.37 kcal/mol) > $\Delta E_{S-T, Mg-Cl}$ (–1.63 kcal/mol, –5.17 kcal/mol) > $\Delta E_{S-T, Mg-Br}$ (–1.63 kcal/mol, –5.17 kcal/mol) and $\Delta E_{S-T, Ca-F}$

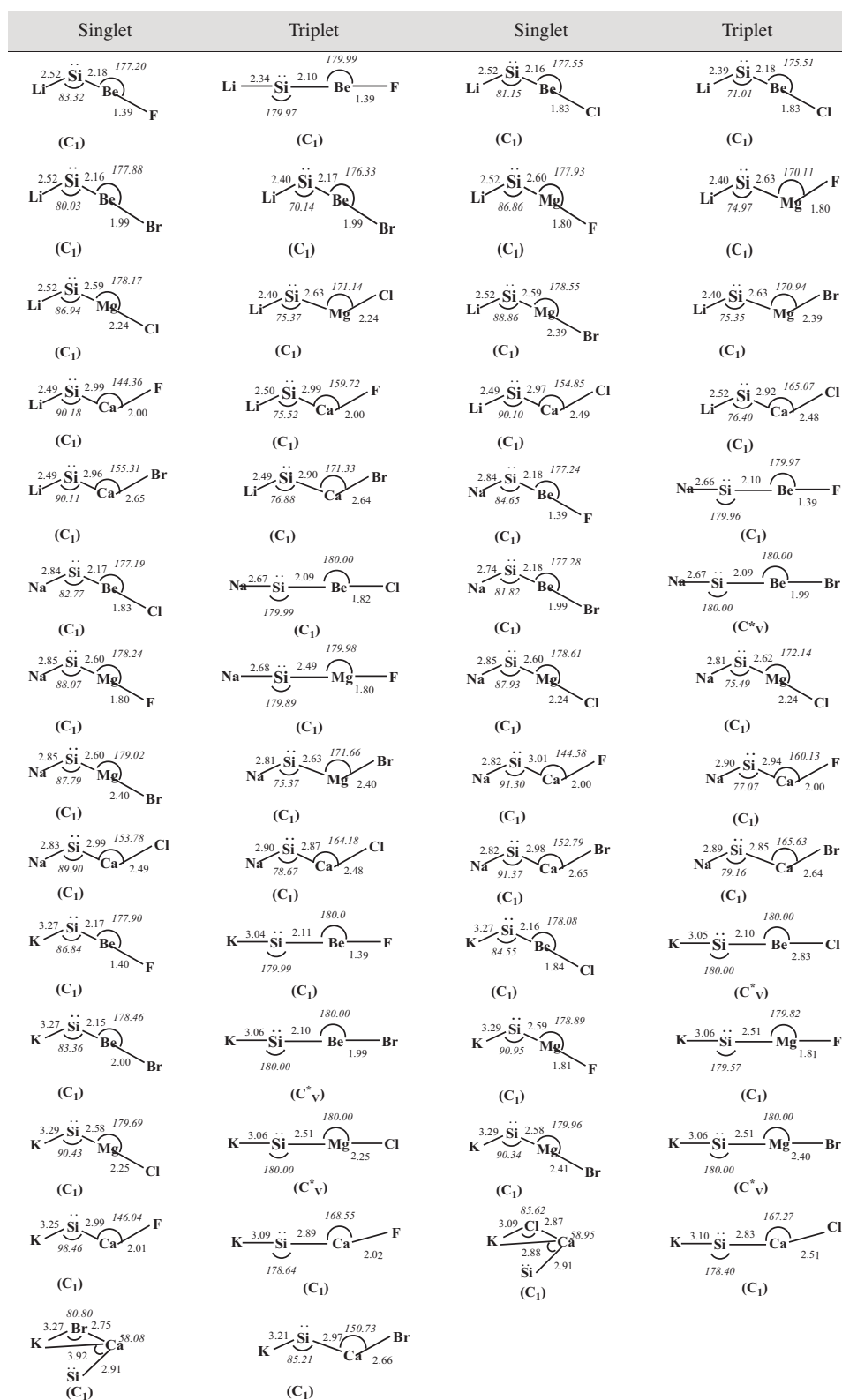


Figure 1. Geometrical parameters of M-Si-M'-X with bond lengths (Å) and bond angles (°) optimized at B3LYP/6-311++G** (M = Li, Na, K and M' = Be, Mg, Ca, and X = F, Cl and Br).

Table 1. Relative energies (kcal/mol) for silylenes (Series 1), singlet (1s-Be-X, 1s-Mg-X, and 1s-Ca-X), and triplet states (1t-Be-X, 1t-Mg-X, and 1t-Ca-X), where X = F, Cl, Br, calculated at two levels of theory; along with B3LYP/6-311++G** computed dipole moments (D) and vibrational zero point energies (kcal/mol).

Structures	Dipole moments (D) B3LYP /6-311++G**	Vibrational zero point energies (kcal/mol) B3LYP/6-311++G**	Relative energies		
			B3LYP /6-311++G**	QCISD(T) /6-311++G**	CCSD(T) /6-311++G**
1s-Be-F	6.11	3.73	10.33	9.10	9.11
1s-Be-Cl	6.16	3.08	2.93	3.98	3.94
1s-Be-Br	6.16	2.84	2.91	3.85	3.81
1t-Be-F	8.42	3.90	0	0	0
1t-Be-Cl	5.78	2.98	0	0	0
1t-Be-Br	5.74	2.75	0	0	0
1s-Mg-F	6.87	2.42	3.48	5.59	5.46
1s-Mg-Cl	7.21	2.04	3.35	5.42	5.31
1s-Mg-Br	7.22	1.88	3.32	5.39	5.28
1t-Mg-F	6.62	2.37	0	0	0
1t-Mg-Cl	6.87	1.98	0	0	0
1t-Mg-Br	6.89	1.82	0	0	0
1s-Ca-F	5.60	2.02	5.08	9.50	9.48
1s-Ca-Cl	6.21	1.64	4.94	8.64	8.60
1s-Ca-Br	6.43	1.50	4.94	8.30	8.25
1t-Ca-F	5.14	1.92	0	0	0
1t-Ca-Cl	5.79	1.53	0	0	0
1t-Ca-Br	5.66	1.37	0	0	0

(-5.60 kcal/mol, -9.92 kcal/mol) > ΔE_{S-T} , Ca-Cl (-5.56 kcal/mol, -8.81 kcal/mol) > ΔE_{S-T} , Ca-Br (-5.56 kcal/mol, -8.80 kcal/mol) (Table 2). Evidently, fluorine has an extraordinary effect on ΔE_{S-T} , Mg-F, which is due to the fair orbital size difference between Na and Mg. On the other hand, Na and Mg are in the same period and their ionic radii are approximately near to each other ($\text{Na}^+ = 1.16 \text{ \AA}$, $\text{Mg}^{2+} = 0.85 \text{ \AA}$).⁴² It could be a reasonable reason for stability of ΔE_{S-T} , Be-F in Li-Si-Be-F. Interestingly, ΔE_{S-T} , Mg-F in Na-Si-Mg-F and ΔE_{S-T} , Ca-F in Li-Si-Be-F show fair triplet stability structures. In Series 3, singlet-triplet energy gaps have a manifest consistency trend at DFT and single-point levels of theory (Table 3). Clearly, these compounds with the highest electropositive substituent (M = K), have the most stable triplets relative to 1t-X and 2t-X. Energy gaps between 3s-M'-X and 3t-M'-X, calculated at B3LYP/6-311++G** and QCISD(T)/6-311++G** levels of theory, appear as: ΔE_{S-T} , Be-F (-12.44 kcal/mol, -12.29 kcal/mol) > ΔE_{S-T} , Be-Cl (-11.37 kcal/mol, -11.79 kcal/mol) > ΔE_{S-T} , Be-Br (-11.18 kcal/mol, -11.41 kcal/mol) and ΔE_{S-T} , Mg-F (-11.91 kcal/mol, -12.23 kcal/mol) > ΔE_{S-T} , Mg-Cl (-11.63 kcal/mol, -12.18 kcal/mol) > ΔE_{S-T} , Mg-Br (-11.58 kcal/mol, -12.09 kcal/mol) and ΔE_{S-T} , Ca-F (-14.15 kcal/mol, -13.64 kcal/mol) > ΔE_{S-T} , Ca-Cl (-9.43 kcal/mol, -8.79 kcal/mol) > ΔE_{S-T} , Ca-Br (-2.41 kcal/mol, -7.88 kcal/mol) (Table 3). Evidently,

Table 2. Relative energies (kcal/mol) for silylenes (Series 2), singlet ($2s\text{-Be-X}$, $2s\text{-Mg-X}$, and $2s\text{-Ca-X}$), and triplet states ($2t\text{-Be-X}$, $2t\text{-Mg-X}$, and $2t\text{-Ca-X}$), where X = F, Cl, Br, calculated at two levels of theory; along with B3LYP/6-311++G** computed dipole moments (D) and vibrational zero point energies (kcal/mol).

Structures	Dipole moments (D) B3LYP /6-311++G**	Vibrational zero point energies (kcal/mol) B3LYP/6-311++G**	Relative energies		
			B3LYP /6-311++G**	QCISD(T) /6-311++G**	CCSD(T) /6-311++G**
$2s\text{-Be-F}$	6.26	3.43	7.33	8.26	8.26
$2s\text{-Be-Cl}$	6.41	2.78	7.30	8.11	8.14
$2s\text{-Be-Br}$	6.46	2.53	7.09	7.84	7.85
$2t\text{-Be-F}$	9.89	3.51	0	0	0
$2t\text{-Be-Cl}$	10.23	2.87	0	0	0
$2t\text{-Be-Br}$	10.39	2.63	0	0	0
$2s\text{-Mg-F}$	7.09	2.11	7.53	8.37	8.40
$2s\text{-Mg-Cl}$	7.45	1.74	1.63	5.17	5.03
$2s\text{-Mg-Br}$	7.46	1.56	1.63	5.17	5.03
$2t\text{-Mg-F}$	10.87	2.18	0	0	0
$2t\text{-Mg-Cl}$	8.12	1.62	0	0	0
$2t\text{-Mg-Br}$	8.18	1.46	0	0	0
$2s\text{-Ca-F}$	5.63	1.68	5.60	9.92	9.93
$2s\text{-Ca-Cl}$	7.29	1.31	5.56	8.81	8.80
$2s\text{-Ca-Br}$	6.95	1.19	5.56	8.80	8.80
$2t\text{-Ca-F}$	5.54	1.60	0	0	0
$2t\text{-Ca-Cl}$	6.37	1.23	0	0	0
$2t\text{-Ca-Br}$	6.35	1.10	0	0	0

the structures with the most electronegative substituents (like Li-Si-Be-F and K-Si-Ca-F) have the smallest singlet-triplet energy gaps. The Frontier molecular orbitals for singlet and triplet states of these structures are obtained (Figure 2).

The declining trend of LUMO-HOMO energy gaps ($\Delta E_{HOMO-LUMO}$) is as follows: Series 1 \geq Series 2 $>$ Series 3 (Table 4).

An inspection of the calculated LUMO-HOMO energy gaps ($\Delta E_{HOMO-LUMO}$) in all singlet silylenes also seems to suggest that this parameter is dictated by the size of the angle formed by the two substituents bound to the central atom.⁴³

The magnitude of divalent bond angle is one of the considerable parameters affecting the ΔE_{S-T} .³⁰ Variations in the Li-Si-M' divalent angles of singlet $1s\text{-X}$ and triplet $1t\text{-X}$ as a function of X are negligible and in all of them the angles are bent (except in the case of triplet Li-Si-Be-F). Among our 54 silylene isomers, only two singlet structures, K-Si-Ca-Cl and K-Si-Ca-Br, undergo rearrangement upon optimization, forming rather long linkages from K to Ca (Figure 1).

In Series 2, four triplet structures are linear (Na-Si-Be-F, Na-Si-Be-Cl, Na-Si-Be-Br, and Na-Si-Mg-

Table 3. Relative energies (kcal/mol) for silylenes (Series 3), singlet ($3s\text{-Be-X}$, $3s\text{-Mg-X}$, and $3s\text{-Ca-X}$), and triplet states ($3t\text{-Be-X}$, $3t\text{-Mg-X}$, and $3t\text{-Ca-X}$), where X = F, Cl, Br, calculated at two levels of theory; along with B3LYP/6-311++G** computed dipole moments (D) and vibrational zero point energies (kcal/mol).

Structures	Dipole moments (D)	Vibrational zero point energies (kcal/mol)	Relative energies		
			B3LYP /6-311++G**	QCISD(T) /6-311++G**	CCSD(T) /6-311++G**
	B3LYP /6-311++G**	(kcal/mol) B3LYP/6-311++G**			
$3s\text{-Be-F}$	8.90	3.29	12.44	12.29	12.31
$3s\text{-Be-Cl}$	9.15	2.64	11.37	11.79	11.81
$3s\text{-Be-Br}$	9.23	2.40	11.18	11.41	11.44
$3t\text{-Be-F}$	12.49	3.42	0	0	0
$3t\text{-Be-Cl}$	12.98	2.80	0	0	0
$3t\text{-Be-Br}$	13.21	2.54	0	0	0
$3s\text{-Mg-F}$	9.77	1.99	11.91	12.23	12.28
$3s\text{-Mg-Cl}$	10.15	1.60	11.63	12.18	12.23
$3s\text{-Mg-Br}$	10.22	1.45	11.58	12.09	12.14
$3t\text{-Mg-F}$	13.91	2.06	0	0	0
$3t\text{-Mg-Cl}$	14.56	1.71	0	0	0
$3t\text{-Mg-Br}$	14.68	1.55	0	0	0
$3s\text{-Ca-F}$	8.54	1.57	14.15	13.64	13.77
$3s\text{-Ca-Cl}$	3.84	1.36	9.43	8.79	8.92
$3s\text{-Ca-Br}$	3.45	1.21	2.41	7.88	7.97
$3t\text{-Ca-F}$	10.12	1.54	0	0	0
$3t\text{-Ca-Cl}$	12.17	1.25	0	0	0
$3t\text{-Ca-Br}$	11.85	0.99	0	0	0

F) and the others are bent. In all compounds of these structures, the Si-M'-X bond angle is bent to a degree that is (except in the case of one triplet) a function of the atomic size of X: Br \approx Cl > F.

All compounds with $3t\text{-X}$ structures are linear, which confirms the stability of the triplet states for these structures with M = K relative to the others (except in the case of one triplet).

Although the Si-M' bond length does vary significantly across this series of structures, the M'-X bond lengths notably as the size of the halogen substituent increases (Br > Cl > F). Most of the species have C_1 point groups, except for those that have $C_{\infty v}$ point groups (Figure 1).

Isodesmic reactions 1, 2, and 3 are employed to evaluate the sum of electronic and thermal enthalpies of silylenes with different substituents. Clearly, every triplet silylene ($1t\text{-X}$, $2t\text{-X}$) with more electronegative β -substituents appears slightly more stable than its corresponding triplets with less electronegative ones (Table 5).

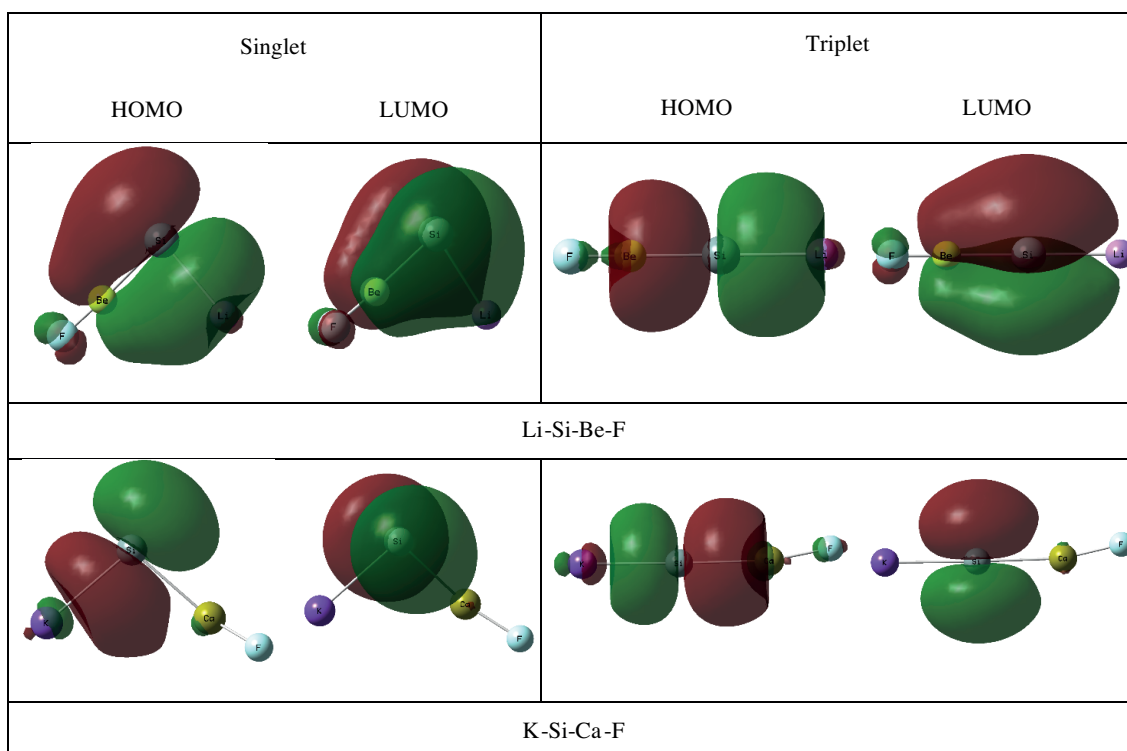


Figure 2. Shapes of selected molecular orbitals for Li-Si-Be-F and K-Si-Ca-F singlet and triplet silylenes.

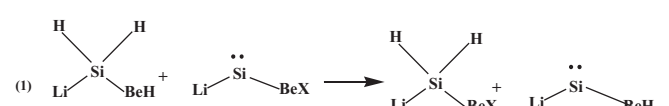
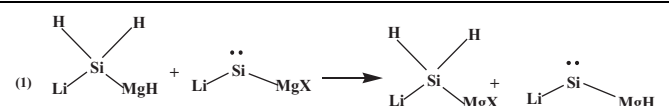
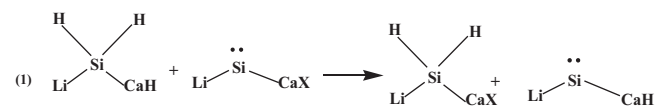
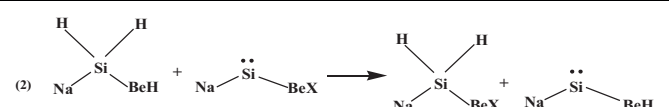
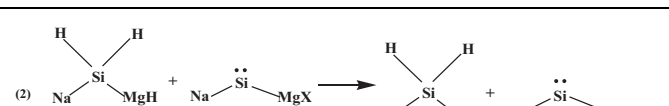
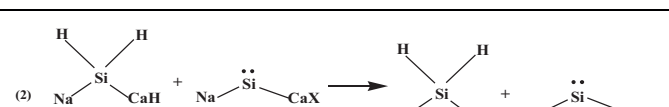
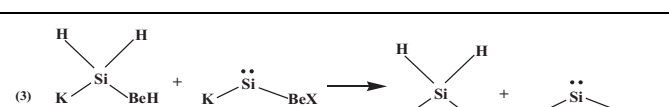
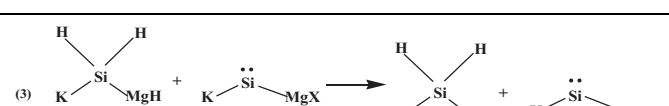
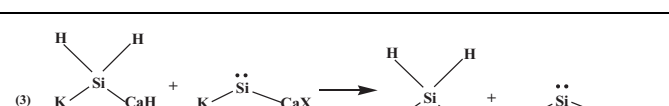
Table 4. LUMO-HOMO energy gaps ($\Delta E_{HOMO-LUMO}$) for singlet silylenes, at B3LYP/6-311++G**.

Structures 1	$\Delta E_{HOMO-LUMO}$	Structures 2	$\Delta E_{HOMO-LUMO}$	Structures 3	$\Delta E_{HOMO-LUMO}$
$1s-Be-F$	36.39	$2s-Be-F$	35.14	$3s-Be-F$	28.86
$1s-Be-Cl$	36.39	$2s-Be-Cl$	34.51	$3s-Be-Cl$	28.86
$1s-Be-Br$	36.39	$2s-Be-Br$	34.51	$3s-Be-Br$	28.86
$1s-Mg-F$	35.76	$2s-Mg-F$	34.51	$3s-Mg-F$	28.23
$1s-Mg-Cl$	36.39	$2s-Mg-Cl$	34.51	$3s-Mg-Cl$	28.86
$1s-Mg-Br$	36.39	$2s-Mg-Br$	34.51	$3s-Mg-Br$	28.23
$1s-Ca-F$	34.51	$2s-Ca-F$	33.88	$3s-Ca-F$	28.23
$1s-Ca-Cl$	34.51	$2s-Ca-Cl$	33.25	$3s-Ca-Cl$	25.10
$1s-Ca-Br$	34.51	$2s-Ca-Br$	33.88	$3s-Ca-Br$	25.10

The stability of a reactive species requires its resistance to isomerization, which necessitates identifying and calculating energy barriers for such processes.⁴⁴ One of the most important reactions of silylenes is insertion into the hydrogen molecule. Accordingly, the insertion reactions of hydrogen into silylenes afford the dihydrido-silane (Scheme 2).

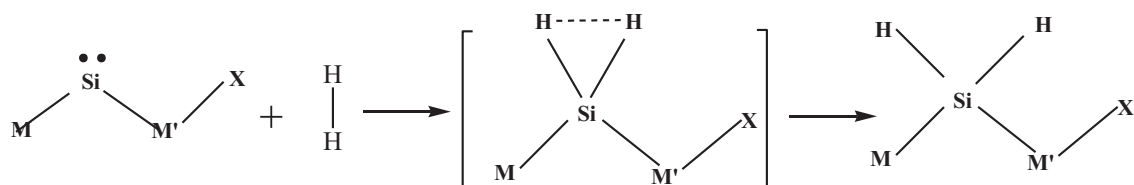
In close analogy, every singlet silylene can undergo an intramolecular H-H bond activation.¹⁷ Table 6 shows the heats of hydrogenation (ΔH_H) and energy barriers of silylenes hydrogenation. Strikingly, $1s-Ca-Br$, $2s-Ca-Br$, and $3s-Ca-F$ are the most capable of activating dihydrogen, likely due to their relatively small singlet-triplet energy gaps.

Table 5. Isodesmic reactions showing the relative thermal energies of singlet (ΔE_S) and triplet (ΔE_T) silylenes, in kcal/mol, at B3LYP/6-311 ++G** level, where X = F, Cl, Br.

Isodesmic reactions	X	Relative thermal energies	
		ΔE_S^a	ΔE_T^b
(1) 	F	-8.4	-12.8
	Cl	-9.4	-17.4
	Br	-9.9	-24.5
(1) 	F	-9.7	22.7
	Cl	-9.7	13.4
	Br	-9.8	12.2
(1) 	F	-7.1	-1.7
	Cl	-5.9	-9.5
	Br	-5.7	-9.7
(2) 	F	-8.8	-4.9
	Cl	-9.6	-6.0
	Br	-10.1	-10.7
(2) 	F	-10.0	-9.9
	Cl	-10.0	-4.1
	Br	-10.1	-4.1
(2) 	F	-10.3	-8.6
	Cl	-5.9	-8.8
	Br	-5.7	-8.9
(3) 	F	-7.5	-10.1
	Cl	-9.2	17.7
	Br	-9.7	-2.1
(3) 	F	-9.3	-12.0
	Cl	-9.4	-2-2
	Br	-9.5	-3.8
(3) 	F	-11.1	-22.5
	Cl	-15.1	-19.6
	Br	-14.3	-12.1

^a Singlet germlylenes are employed in both sides of the isodesmic reactions.^b Triplet germlylenes are employed in both sides of the isodesmic reactions.

In 2010, Nyíri studied hydrogen insertion into SiH₂. The reaction proceeded via a concerted transition state in which the vacant *p*-orbital and the lone pair on the silicon atom interacted with the σ -bonding and σ^* -antibonding orbitals of hydrogen, respectively, forming a three-membered ring structure.⁴⁵ In contrast, our reactions indicate a surprisingly different character. In the transition state, both or one of the hydrogen atoms interact with the silicon center. Interestingly, the ionic bond pair electron of silicon center (attached to M) is more active than its free lone pair and interacts with one of the hydrogens. Hence, at the same time, the Si-M



Scheme 2. Direct insertion of hydrogen into M-Si-M'-X species, where M = Li, Na, K; M' = Be, Mg, Ca; and X = F, Cl, Br.

Table 6. Heats of hydrogenation (ΔH_H^a) and hydrogen activation barrier of M-Si-M'-X species (ΔE_a^\ddagger / kcal mol⁻¹) at B3LYP/6-311++G** level (M = Li, Na, K; M' = Be, Mg, Ca; and X = F, Cl, Br).

Series 1	ΔH_H^a	ΔE_a^\ddagger	Series 2	ΔH_H^a	ΔE_a^\ddagger	Series 3	ΔH_H^a	ΔE_a^\ddagger
1 _{s-Be-F}	-54.96	-28.61	2 _{s-Be-F}	-54.08	-41.39	3 _{s-Be-F}	-55.57	-31.53
1 _{s-Be-Cl}	-53.94	-33.41	2 _{s-Be-Cl}	-53.19	-45.33	3 _{s-Be-Cl}	-54.42	-34.13
1 _{s-Be-Br}	-53.44	-34.82	2 _{s-Be-Br}	-52.75	-45.37	3 _{s-Be-Br}	-53.89	-35.15
1 _{s-Mg-F}	-54.32	-41.37	2 _{s-Mg-F}	-54.45	-45.16	3 _{s-Mg-F}	-55.50	-51.36
1 _{s-Mg-Cl}	-54.28	-41.44	2 _{s-Mg-Cl}	-53.39	-33.08	3 _{s-Mg-Cl}	-55.44	-51.45
1 _{s-Mg-Br}	-54.21	-41.35	2 _{s-Mg-Br}	-53.33	-42.94	3 _{s-Mg-Br}	-55.33	-51.58
1 _{s-Ca-F}	-56.27	-47.31	2 _{s-Ca-F}	-53.88	-49.00	3 _{s-Ca-F}	-55.80	-54.57
1 _{s-Ca-Cl}	-57.45	-50.60	2 _{s-Ca-Cl}	-58.25	-48.12	3 _{s-Ca-Cl}	-54.81	-49.80
1 _{s-Ca-Br}	-57.67	-50.69	2 _{s-Ca-Br}	-58.45	-50.75	3 _{s-Ca-Br}	-55.56	-50.20

^aMSiM'X + H₂ → HSiH₂M'X

bond splits and the new Si-H bond forms. The results unambiguously support that one or two new Si-H bonds form in the transition state while the Si-M bond splits. Generally, the mechanisms of all the reactions are very similar to each other.

Finally, the NBO atomic charges are computed for singlet and triplet states of silylene species (Table 7, Supplementary information). Clearly, halogens have some effects on NBO atomic charges of triplet silicon atoms with the trend of: M-Si-M'-F > M-Si-M'-Cl > M-Si-M'-Br, showing the influence of electronegative substituents on the stability of triplet silylenes (Table 7).

The results show that charges on all linear triplet silylenes are less than those of the corresponding singlet species (Table 7). In fact, silicon atoms in singlets tend to have their nonbonding electrons in the atomic orbitals with higher *s*-character. Consequently, electropositive substituents transfer charge from their corresponding Si-M and Si-M' bonding orbitals with higher *p*-character to the partially populated *s*-type orbital on the silicon atom.

The results also show that more linear molecules (all triplet species) have lower *p*-character than their corresponding singlets (Table 8). For example, Na-Si-Be-Br (t) with lower *p*-character (*s*¹ *p*¹) is more linear than its corresponding singlet (*s*¹ *p*^{5.54} *d*^{0.01}). Consequently, the *s*-character may be held responsible for the choice of the silicon ground state multiplicity (Table 8).

Furthermore, the stabilization energies for the intermolecular interactions (LP_X → σ*_{Si-M'}) are calculated using NBO analysis. Interestingly, except for species with M' = Be, stabilization energies trends fall in the order of: M-Si-M'-Cl > M-Si-M'-Br > M-Si-M'-F. However, in species with M' = Be, the trend reduces as a function of electronegativity of halogens (M-Si-M'-Br > M-Si-M'-Cl > M-Si-M'-F) (Table 9).

Table 7. The B3LYP/6-311++G** calculated NBO atomic charges for M–Si–M'–X species, where M = Li, Na, K; M' = Be, Mg, Ca; and X = F, Cl, Br.

Structures	Si	F	Structures	Si	Cl	Structures	Si	Br
Li–Si–Be–F (s)	-0.55	-0.72	<i>Li–Si–Be–Cl (s)</i>	-0.45	-0.47	<i>Li–Si–Be–Br (s)</i>	-0.43	-0.41
Li–Si–Be–F (t)	-0.96	-0.71	<i>Li–Si–Be–Cl (t)</i>	-0.49	-0.47	<i>Li–Si–Be–Br (t)</i>	-0.84	-0.41
Na–Si–Be–F (s)	-0.97	-0.71	<i>Na–Si–Be–Cl (s)</i>	-0.48	-0.48	<i>Na–Si–Be–Br (s)</i>	-0.46	-0.42
Na–Si–Be–F (t)	-0.99	-0.72	<i>Na–Si–Be–Cl (t)</i>	-0.88	-0.48	<i>Na–Si–Be–Br (t)</i>	-0.86	-0.42
K–Si–Be–F (s)	-0.67	-0.67	<i>K–Si–Be–Cl (s)</i>	-0.55	-0.50	<i>K–Si–Be–Br (s)</i>	-0.53	-0.44
K–Si–Be–F (t)	-1.02	-0.72	<i>K–Si–Be–Cl (t)</i>	-0.91	-0.49	<i>K–Si–Be–Br (t)</i>	-0.89	-0.44
Li–Si–Mg–F (s)	-0.78	-0.87	<i>Li–Si–Mg–Cl (s)</i>	-0.71	-0.71	<i>Li–Si–Mg–Br (s)</i>	-0.70	-0.66
Li–Si–Mg–F (t)	-0.77	-0.87	<i>Li–Si–Mg–Cl (t)</i>	-0.71	-0.71	<i>Li–Si–Mg–Br (t)</i>	-0.69	-0.66
Na–Si–Mg–F (s)	-0.82	-0.87	<i>Na–Si–Mg–Cl (s)</i>	-0.74	-0.72	<i>Na–Si–Mg–Br (s)</i>	-0.73	-0.67
Na–Si–Mg–F (t)	-1.28	-0.87	<i>Na–Si–Mg–Cl (t)</i>	-0.77	-0.72	<i>Na–Si–Mg–Br (t)</i>	-0.76	-0.67
K–Si–Mg–F (s)	-0.91	-0.87	<i>K–Si–Mg–Cl (s)</i>	-0.82	-0.73	<i>K–Si–Mg–Br (s)</i>	-0.80	-0.68
K–Si–Mg–F (t)	-1.28	-0.87	<i>K–Si–Mg–Cl (t)</i>	-1.19	-0.73	<i>K–Si–Mg–Br (t)</i>	-1.18	-0.68
Li–Si–Ca–F (s)	-0.99	-0.86	<i>Li–Si–Ca–Cl (s)</i>	-0.94	-0.79	<i>Li–Si–Ca–Br (s)</i>	-0.93	-0.77
Li–Si–Ca–F (t)	-0.92	-0.86	<i>Li–Si–Ca–Cl (t)</i>	-0.90	-0.78	<i>Li–Si–Ca–Br (t)</i>	-0.90	-0.76
Na–Si–Ca–F (s)	-1.04	-0.86	<i>Na–Si–Ca–Cl (s)</i>	-0.97	-0.79	<i>Na–Si–Ca–Br (s)</i>	-0.97	-0.77
Na–Si–Ca–F (t)	-0.97	-0.86	<i>Na–Si–Ca–Cl (t)</i>	-0.93	-0.78	<i>Na–Si–Ca–Br (t)</i>	-0.93	-0.76
K–Si–Ca–F (s)	-1.15	-0.86	<i>K–Si–Ca–Cl (s)</i>	-0.91	-0.83	<i>K–Si–Ca–Br (s)</i>	-0.91	-0.80
K–Si–Ca–F (t)	-1.53	-0.87	<i>K–Si–Ca–Cl (t)</i>	-1.46	-0.81	<i>K–Si–Ca–Br (t)</i>	-0.99	-0.77

Evidently, the structures with the most electronegative substituent have the lowest stabilization energies and singlet–triplet energy gaps. It may be due to the better hyperconjugation effect of the F group attached to the M' center ($LP_F \rightarrow \sigma^*_{Si-M'}$) than Cl and Br. As we know F^- is a better base than Cl^- and Br^- . Clearly, fluorine substituent destabilizes M' atoms σ orbitals and the triplets with fluorine substituents appear more stable than the triplets with chlorine and bromine substituents.

4. Conclusion

The effect of several first and second group di-alkaline metal substituents on the singlet–triplet energy separating, multiplicity, and relative stabilities of divalent silylenes with M–Si–M'–X formulation is considered by using B3LYP/6-311++G** as well as the ab initio method QCISD(T)/6-311++G** and CCSD(T)/6-311++G** levels of theory, where M = Li, Na, K; M' = Be, Mg, Ca; and X = F, Cl, Br. Calculations pointed out electropositive substituents must be effective in reduction of the promotion energy and singlet–triplet energy separating to the point that a triplet ground state can be obtained at a reasonable bond angle. Moreover our calculations confirm that K–Si–Ca–X shows the most promise for its lower singlet–triplet energy difference and narrower band gap ($\Delta E_{HOMO-LUMO}$). Furthermore, we find that every triplet alkali-silylene with more electronegative β -substituents appears slightly more stable than its corresponding triplet with less electronegative substituents.

Table 8. The B3LYP/6-311++G** calculated hybridizations for linear triplet M-Si-M'-X species and their corresponding singlets (M = Li, Na, K; M' = Be, Mg, Ca, and X = F, Cl, Br).

Structures	Bond		Structures	Bond		Structures	Bond	
	σ_{M-Si}	$\sigma_{Si-M'}$		σ_{M-Si}	$\sigma_{Si-M'}$		σ_{M-Si}	$\sigma_{Si-M'}$
Li-Si-Be-F(s)	$s^1 p^{47.80} d^{0.11}$	$s^1 p^{8.00} d^{0.02}$	K-Si-Be-F(s)	$s^1 p^{99.99} d^{0.20}$	$s^1 p^{6.88} d^{0.02}$	K-Si-Mg-Cl(s)	$s^1 p^{99.12} d^{0.12}$	$s^1 p^{11.89} d^{0.02}$
Li-Si-Be-F(t)	-	$s^1 p^{1.00} d^{0.00}$	K-Si-Be-F(t)	-	$s^1 p^{4.36} d^{0.00}$	K-Si-Mg-Cl(t)	-	$s^1 p^{6.12} d^{0.00}$
Na-Si-Be-F(s)	$s^1 p^{75.87} d^{0.12}$	$s^1 p^{7.44} d^{0.02}$	K-Si-Be-Cl(s)	$s^1 p^{99.99} d^{0.27}$	$s^1 p^{5.36} d^{0.01}$	K-Si-Mg-Br(s)	$s^1 p^{99.99} d^{0.13}$	$s^1 p^{11.49} d^{0.02}$
Na-Si-Be-F(t)	-	$s^1 p^{4.25} d^{0.00}$	K-Si-Be-Cl(t)	-	$s^1 p^{1.00} d^{0.00}$	K-Si-Mg-Br(t)	-	$s^1 p^{5.91} d^{0.00}$
Na-Si-Be-Cl(s)	$s^1 p^{99.99} d^{0.21}$	$s^1 p^{5.77} d^{0.01}$	K-Si-Be-Br(s)	$s^1 p^{99.99} d^{0.30}$	$s^1 p^{5.04} d^{0.01}$	K-Si-Ca-F(s)	$s^1 p^{99.41} d^{0.06}$	$s^1 p^{15.86} d^{0.01}$
Na-Si-Be-Cl(t)	-	$s^1 p^{1.00} d^{0.00}$	K-Si-Be-Br(t)	-	$s^1 p^{1.00} d^{0.00}$	K-Si-Ca-F(t)	-	$s^1 p^{11.13} d^{0.00}$
Na-Si-Be-Br(s)	$s^1 p^{99.99} d^{0.30}$	$s^1 p^{5.54} d^{0.01}$	K-Si-Mg-F(s)	$s^1 p^{94.13} d^{0.09}$	$s^1 p^{13.93} d^{0.02}$	K-Si-Ca-Cl(s)	$s^1 p^{41.56} d^{0.04}$	$s^1 p^{30.26} d^{0.03}$
Na-Si-Be-Br(t)	-	$s^1 p^{1.00} d^{0.00}$	K-Si-Mg-F(t)	-	$s^1 p^{7.05} d^{0.01}$	K-Si-Ca-Cl(t)	-	$s^1 p^{7.86} d^{0.00}$
Na-Si-Mg-F(s)	$s^1 p^{46.34} d^{0.07}$	$s^1 p^{16.16} d^{0.02}$	Na-Si-Mg-F(t)	-	$s^1 p^{7.14} d^{0.01}$			

Table 9. Calculated second-order perturbation stabilization energies ($E^{(2)}$), for the intermolecular interactions ($LP_X \rightarrow \sigma^*_{Si-M'}$) using NBO analysis at the B3LYP/6-311++G** level of theory for singlet M-Si-M'-X species (M = Li, Na, K; M' = Be, Mg, Ca; and X = F, Cl, Br).

Series 1	donor→acceptor	$E^{(2)}$	Series 2	donor→acceptor	$E^{(2)}$	Series 3	donor→acceptor	$E^{(2)}$
1 _{s-Be-F}	$LP_F \rightarrow \sigma^*_{Si-M'}$	0.14	2 _{s-Be-F}	$LP_F \rightarrow \sigma^*_{Si-M'}$	0.18	3 _{s-Be-F}	$LP_F \rightarrow \sigma^*_{Si-M'}$	0.23
1 _{s-Be-Cl}	$LP_{Cl} \rightarrow \sigma^*_{Si-M'}$	1.49	2 _{s-Be-Cl}	$LP_{Cl} \rightarrow \sigma^*_{Si-M'}$	1.52	3 _{s-Be-Cl}	$LP_{Cl} \rightarrow \sigma^*_{Si-M'}$	1.46
1 _{s-Be-Br}	$LP_{Br} \rightarrow \sigma^*_{Si-M'}$	2.69	2 _{s-Be-Br}	$LP_{Br} \rightarrow \sigma^*_{Si-M'}$	2.70	3 _{s-Be-Br}	$LP_{Br} \rightarrow \sigma^*_{Si-M'}$	2.63
1 _{s-Mg-F}	$LP_F \rightarrow \sigma^*_{Si-M'}$	0.24	2 _{s-Mg-F}	$LP_F \rightarrow \sigma^*_{Si-M'}$	0.21	3 _{s-Mg-F}	$LP_F \rightarrow \sigma^*_{Si-M'}$	0.28
1 _{s-Mg-Cl}	$LP_{Cl} \rightarrow \sigma^*_{Si-M'}$	3.44	2 _{s-Mg-Cl}	$LP_{Cl} \rightarrow \sigma^*_{Si-M'}$	3.49	3 _{s-Mg-Cl}	$LP_{Cl} \rightarrow \sigma^*_{Si-M'}$	3.72
1 _{s-Mg-Br}	$LP_{Br} \rightarrow \sigma^*_{Si-M'}$	2.70	2 _{s-Mg-Br}	$LP_{Br} \rightarrow \sigma^*_{Si-M'}$	1.68	3 _{s-Mg-Br}	$LP_{Br} \rightarrow \sigma^*_{Si-M'}$	3.57
1 _{s-Ca-F}	$LP_F \rightarrow \sigma^*_{Si-M'}$	3.42	2 _{s-Ca-F}	$LP_F \rightarrow \sigma^*_{Si-M'}$	3.49	3 _{s-Ca-F}	$LP_F \rightarrow \sigma^*_{Si-M'}$	3.52
1 _{s-Ca-Cl}	$LP_{Cl} \rightarrow \sigma^*_{Si-M'}$	—	2 _{s-Ca-Cl}	$LP_{Cl} \rightarrow \sigma^*_{Si-M'}$	4.00	3 _{s-Ca-Cl}	$LP_{Cl} \rightarrow \sigma^*_{Si-M'}$	5.84
1 _{s-Ca-Br}	$LP_{Br} \rightarrow \sigma^*_{Si-M'}$	0.57	2 _{s-Ca-Br}	$LP_{Br} \rightarrow \sigma^*_{Si-M'}$	3.57	3 _{s-Ca-Br}	$LP_{Br} \rightarrow \sigma^*_{Si-M'}$	5.57

Acknowledgment

The authors wish to gratefully thank Dr Maryam Koochi for many useful discussions.

References

- Schoeller, W. W.; Sundermann, A.; Reiher, M. *Inorg. Chem.* **1999**, *38*, 29-37.
- Bourissou, D.; Guerret, O.; Gabbai, F. P.; Bertrand, G. *Chem. Rev.* **2000**, *100*, 39-92.
- Mizuhata, Y.; Sasamori, T.; Tokitoh, N. *Chem. Rev.* **2009**, *109*, 3479-3511.
- Sasamori, T.; Tokitoh, N. in *Encyclopedia of Inorganic Chemistry II*; King, R. B., Eds. John Wiley & Sons: Chichester, UK, 2005, pp. 1698-1740.
- Fueno, T. Eds. *The Transition State: A Theoretical Approach*; Gordon and Breach Science Publishers: Langhorne, PA USA, 1999, pp. 147-161.
- Barden, C. J.; Schaefer, H. F. *J. Chem. Phys.* **2000**, *112*, 6515-6516.
- Lee, E. P. F.; Dyke, J. M.; Wright, T. G. *Chem. Phys. Lett.* **2000**, *326*, 143-150.
- Bruce, M. *Chem. Rev.* **1991**, *91*, 197-257.
- Apeloig, Y. in *The Chemistry of Organic Silicon Compounds*; Patai, S.; Rappoport, Z. Eds. Vol. 1, Wiley: New York, NY, USA, 1989, p. 57.
- Vessally, E. *Heteroa. Chem.* **2008**, *19*, 245-251.
- Schaefer, H. F. *Science* **1986**, *231*, 1100-1107.
- Holthausen, M. C.; Koch, W.; Apeloig, Y. *J. Am. Chem. Soc.* **1999**, *121*, 2623-2624.
- Sekiguchi, A.; Tanaka, T.; Ichinohe, M.; Akiyama, K.; Gaspar, P. P. *J. Am. Chem. Soc.* **2008**, *130*, 426-427.
- Grev, R. S.; Schaefer, H. F.; Gaspar, P. P. *J. Am. Chem. Soc.* **1991**, *113*, 5638-5643.
- Luke, B. T.; Pople, J. A.; Krogh-Jespersen, M. B.; Apeloig, Y.; Karni, M.; Chandrasekhar, J.; Schleyer, P. v. R. *J. Am. Chem. Soc.* **1986**, *108*, 270-284.
- Kalcher, J.; Sax, A. F. *J. Mol. Struct. (THEOCHEM)* **1992**, *253*, 287-302.
- Krogh-Jespersen, K. *J. Am. Chem. Soc.* **1985**, *107*, 537-543.

18. Colvin, M. E.; Schaefer, H. F.; Bicerano, J. *J. Chem. Phys.* **1985**, *83*, 4581-4584.
19. Inoue, Sh.; Ichinohe, M.; Sekiguchi, A. *Organometallics* **2008**, *27*, 1358-1360.
20. Nefedov, O. M.; Egorov, M. P.; Ioffe, A. I.; Menchikov, L. G.; Zuev, P. S.; Minkin, V. I.; Simkin, Ya. B.; Glukhovtsev, M. N. *Pure Appl. Chem.* **1992**, *64*, 265-314.
21. Schwartz, R. L.; Davico, G. E.; Ramond, T. M.; Lineberger, W. C. *J. Phys. Chem.* **1999**, *103*, 8213-8221.
22. Zhu, Z.; Bally, T.; Stracener, L. L.; McMahon, R. J. *J. Am. Chem. Soc.* **1999**, *121*, 2863-2874.
23. Wang, Y.; Yuzawa, T.; Hamaguchi, H.; Toscano, J. P. *J. Am. Chem. Soc.* **1999**, *121*, 2875-2882.
24. Wang, Y.; Toscano, J. P. *J. Am. Chem. Soc.* **2000**, *122*, 4512-4513.
25. Gordon, M. S. *Chem. Phys. Lett.* **1985**, *114*, 348-352.
26. Kassaei, M. Z.; Musavi, S. M.; Ghambarian, M. *J. Organomet. Chem.* **2006**, *691*, 1845-1856.
27. Razuvaev, G. A.; Gribov, B. G.; Domrachev, G. A.; Salamatin, B. A. In *Metalloorganicheskie soedineniya v elektronike (Organometallic Compounds in Electronics)*, Nauka: Moscow, USSR, 1972.
28. Gribov, B. G.; Domrachev, G. A.; Zhuk, B. V.; Kaverin, B. S.; Kozyrkin, B. I.; Mel'nikov, V. V.; Suvorova, O. N. In *Precipitation of Films and Covers by Decomposition of Metalloorganic Compounds*. Moscow, USSR: Science, 1981, p. 322.
29. Kassaei, M. Z.; Buazar, F.; Soleimani-Amiri, S. *J. Mol. Struct. (THEOCHEM)* **2008**, *866*, 52-57.
30. Kendall, R. A.; Jr. Dunning, T. H.; Harrison, R. J. *J. Chem. Phys.* **1992**, *96*, 6796-6806.
31. Yan, Z.; Truhlar, D. G. *Theor. Chem. Account.* **2008**, *120*, 215-241.
32. Hehre, W. J.; Radom, L.; Schleyer, P. v. R.; Pople, J. A. *Ab Initio Molecular Orbital Theory*. John Wiley and Sons: New York, NY, USA, 1986.
33. Becke, A. D. *Phys. Rev.* **1988**, *38*, 3098.
34. Becke, A. D. *J. Chem. Phys.* **1993**, *98*, 5648-5652.
35. Lee, C.; Yang, W.; Parr, R. G. *Phys. Rev.* **1988**, *37*, 785.
36. Schmidt, M. W.; Baldridge, K. K.; Boatz, J. A.; Elbert, S. T.; Gordon, M. S.; Jensen, J. H.; Koseki, S.; Matsunaga, N.; Nguyen, K. A.; Su, S. J.; et al. *J. Comput. Chem.* **1993**, *14*, 1347-1363.
37. Sobolewski, A. L.; Domcke, W. *J. Phys. Chem. A* **2002**, *106*, 4158-4167.
38. Parr, R. G.; Yang, W. *Density Functional Theory of Atoms and Molecules*. Oxford University Press: New York, NY, USA, 1989.
39. Hoffmann, R.; Schleyer, P. v. R.; Schaefer, H. F. *Angew. Chem. Int. Ed.* **2008**, *47*, 7164-7167.
40. Sulzbach, H. M.; Bolton, E.; Lenoir, D.; Schleyer, P. v. R.; Schaefer, H. F. *J. Am. Chem. Soc.* **1996**, *118*, 9908-9914.
41. Bundhun, A.; Abdallah, H. H.; Ramasami, P.; Schaefer, H. F. *J. Phys. Chem. A* **2010**, *114*, 13198-13212.
42. Ward, S. G.; Taylor, R. C. In *Metal-Based Anti-Tumor Drugs*; Gielen, M. F. Ed., Freund Publ.: London, UK, 1988.
43. Burgert, B.; Driess, M. In *Functional Molecular Silicon Compounds II*. Springer International Publishing: New York, NY, USA, 2013, pp. 85-123.
44. Moss, R. A.; Fantina, M. E. *J. Am. Chem. Soc.* **1978**, *100*, 6788-6790.
45. Nyíri, K. Szilvási, T.; Veszprémi, T. *Dalton Trans.* **2010**, *39*, 9347-9352.

Supplementary Information

for

New triplet silylenes M–Si–M'–X along with some unusual cyclic forms (M = Li, Na, and K; M' = Be, Mg, and Ca; X = F, Cl, and Br)

Samaneh ASHENAGAR¹, Mohamad Zaman KASSAEE^{1,2,*}

¹Department of Chemistry, Tarbiat Modares University, Tehran, Iran

²Department of Chemical and Biomolecular Engineering, Vanderbilt University, Nashville, TN, USA

*Correspondence: mohamad.z.kassae@vanderbilt.edu

<u>Contents</u>	<u>Page</u>
Table S1. Cartesian coordinates for all calculated structures.	27
Figure S1. Shapes of selected molecular orbitals for singlet silylenes (Series 1).	81
Figure S2. Shapes of selected molecular orbitals for singlet silylenes (Series 2).	83
Figure S3. Shapes of selected molecular orbitals for singlet silylenes (Series 3).	85

Table S1. B3LYP/6-311++G** calculated xyz coordinates for structures studied in this work

B3LYP/6-311++G.**

Li-Si-Be-F (s)

HF = -411.6886871 (a.u.)

Minimum vibrational frequencies ($\nu_{\min}/\text{cm}^{-1}$) = 96.7254

Standard orientation:

Center	Atomic	Atomic	Coordinates (Angstroms)		
Number	Number	Type	X	Y	Z
1	14	0	1.339483	-0.446019	-0.000003
2	4	0	-0.814493	-0.103457	0.000005
3	3	0	1.443268	2.074694	0.000002
4	9	0	-2.202733	0.048223	0.000002

Li-Si-Be-F (t)

HF = -411.7053947 (a.u.)

Minimum vibrational frequencies ($\nu_{\min}/\text{cm}^{-1}$) = 54.2867

Standard orientation:

Center Number	Atomic Number	Atomic Type	Coordinates (Angstroms)		
			X	Y	Z
1	4	0	-1.011933	-0.000068	0.000064
2	3	0	3.445948	0.000668	0.000006
3	9	0	-2.404521	0.000168	-0.000016
4	14	0	1.096470	-0.000232	-0.000009

Li-Si-Mg-F (s)

HF = -597.0246238 (a.u.)

Minimum vibrational frequencies ($\nu_{\min}/\text{cm}^{-1}$) = 78.4841

Standard orientation:

Center Number	Atomic Number	Atomic Type	Coordinates (Angstroms)		
			X	Y	Z
1	12	0	-0.741870	-0.083468	-0.000162
2	3	0	2.039406	2.081613	0.000010
3	9	0	-2.540315	0.098439	0.000127
4	14	0	1.831933	-0.437798	0.000055

Li-Si-Mg-F (t)

HF = -597.0301457 (a.u.)

Minimum vibrational frequencies ($\nu_{\min}/\text{cm}^{-1}$) = 82.3374

Standard orientation:

Center Number	Atomic Number	Atomic Type	Coordinates (Angstroms)		
			X	Y	Z
1	12	0	-0.717842	-0.001456	-0.000135
2	3	0	1.624324	1.990699	0.000042
3	9	0	-2.523673	-0.038737	0.000105
4	14	0	1.889585	-0.400428	0.000039

Li-Si-Ca-F (s)

HF = -1074.5280646 (a.u.)

Minimum vibrational frequencies ($\nu_{\min}/\text{cm}^{-1}$) = 45.7622

Standard orientation:

Center Number	Atomic Number	Atomic Type	Coordinates (Angstroms)		
			X	Y	Z
1	20	0	-0.749313	-0.082820	-0.356840
2	3	0	2.511507	2.042573	-0.020325
3	9	0	-2.554461	0.162322	0.489793
4	14	0	2.174421	-0.423730	0.199260

Li-Si-Ca-F (t)

HF = -1074.5360852 (a.u.)

Minimum vibrational frequencies ($\nu_{\min}/\text{cm}^{-1}$) = 40.6785

Standard orientation:

Center Number	Atomic Number	Atomic Type	Coordinates (Angstroms)		
			X	Y	Z
1	20	0	-0.689662	0.094370	-0.103344
2	3	0	2.092531	2.025766	0.103237
3	9	0	-2.666426	-0.147165	0.136225
4	14	0	2.250963	-0.474302	0.037939

Na-Si-Be-F (s)

HF = -566.4710047 (a.u.)

Minimum vibrational frequencies ($\nu_{\min}/\text{cm}^{-1}$) = 62.8602

Standard orientation:

Center Number	Atomic Number	Atomic Type	Coordinates (Angstroms)		
			X	Y	Z
1	4	0	1.306518	0.064353	0.000108
2	11	0	-1.893218	-1.146978	-0.000063
3	9	0	2.486682	-0.682010	0.000241
4	14	0	-0.484344	1.321245	-0.000137

Na-Si-Be-F (t)

HF = -566.4828386 (a.u.)

Minimum vibrational frequencies ($\nu_{\min}/\text{cm}^{-1}$) = 16.0316

Standard orientation:

Center Number	Atomic Number	Atomic Type	Coordinates (Angstroms)		
			X	Y	Z
1	4	0	1.827184	-0.000089	0.000234
2	11	0	-2.945424	0.000369	0.000006
3	9	0	3.221641	0.000368	-0.000057
4	14	0	-0.278846	-0.000501	-0.000035

Na-Si-Mg-F (s)

HF = -751.8067368 (a.u.)

Minimum vibrational frequencies ($\nu_{\min}/\text{cm}^{-1}$) = 51.8068

Standard orientation:

Center Number	Atomic Number	Atomic Type	Coordinates (Angstroms)		
			X	Y	Z
1	12	0	-1.227991	0.151586	-0.000035
2	11	0	2.271412	-1.322418	0.000003
3	9	0	-2.879711	-0.584374	0.000040
4	14	0	1.119125	1.284781	0.000002

Na-Si-Mg-F (t)

HF = -751.8188336 (a.u.)

Minimum vibrational frequencies ($\nu_{\min}/\text{cm}^{-1}$) = 25.1896

Standard orientation:

Center Number	Atomic Number	Atomic Type	Coordinates (Angstroms)		
			X	Y	Z
1	12	0	1.645389	-0.000084	-0.000001
2	11	0	-3.533268	-0.001329	0.000000
3	9	0	3.449502	-0.000948	0.000001
4	14	0	-0.851731	0.001725	0.000000

Na-Si-Ca-F (s)

HF = -1229.3090645 (a.u.)

Minimum vibrational frequencies ($\nu_{\min}/\text{cm}^{-1}$) = 31.7867

Standard orientation:

Center Number	Atomic Number	Atomic Type	Coordinates (Angstroms)		
			X	Y	Z
1	20	0	-1.229628	-0.131024	-0.354633
2	11	0	2.674654	1.327825	-0.007910
3	9	0	-2.898072	0.606163	0.487809
4	14	0	1.518144	-1.245791	0.199243

Na-Si-Ca-F (t)

HF = -1229.3179579 (a.u.)

Minimum vibrational frequencies ($\nu_{\min}/\text{cm}^{-1}$) = 30.0529

Standard orientation:

Center Number	Atomic Number	Atomic Type	Coordinates (Angstroms)		
			X	Y	Z
1	20	0	-1.028290	-0.004606	-0.073103
2	11	0	2.298781	1.480472	0.017918
3	9	0	-3.004745	0.282956	0.095856
4	14	0	1.594422	-1.338547	0.028733

K-Si-Be-F (s)

HF = -1004.1074171 (a.u.)

Minimum vibrational frequencies ($\nu_{\min}/\text{cm}^{-1}$) = 47.1234

Standard orientation:

Center Number	Atomic Number	Atomic Type	Coordinates (Angstroms)		
			X	Y	Z
1	4	0	-1.801430	-0.161254	0.000161
2	19	0	2.012349	-0.536755	0.000027
3	9	0	-2.685730	-1.248370	-0.000039
4	14	0	-0.489810	1.577049	-0.000057

K-Si-Be-F (t)

HF = -1004.1264386 (a.u.)

Minimum vibrational frequencies ($\nu_{\min}/\text{cm}^{-1}$) = 28.9538

Standard orientation:

Center Number	Atomic Number	Atomic Type	Coordinates (Angstroms)		
			X	Y	Z
1	4	0	0.000131	0.008067	2.505226
2	19	0	-0.000138	-0.008528	-2.661271
3	9	0	0.000203	0.012608	3.903560
4	14	0	0.000020	0.001164	0.386514

K-Si-Mg-F (s)

HF = -1189.4431523 (a.u.)

Minimum vibrational frequencies ($\nu_{\min}/\text{cm}^{-1}$) = 42.0468

Standard orientation:

Center Number	Atomic Number	Atomic Type	Coordinates (Angstroms)		
			X	Y	Z
1	12	0	1.738021	0.052164	0.000001
2	19	0	-2.403202	-0.782231	-0.000023
3	9	0	3.153708	-1.080889	0.000030
4	14	0	-0.255628	1.711744	0.000011

K-Si-Mg-F (t)

HF = -1189.4622034 (a.u.)

Minimum vibrational frequencies ($\nu_{\min}/\text{cm}^{-1}$) = 26.3757

Standard orientation:

Center Number	Atomic Number	Atomic Type	Coordinates (Angstroms)		
			X	Y	Z
1	12	0	2.313263	-0.001755	-0.000006
2	19	0	-3.264069	-0.003135	0.000001
3	9	0	4.123392	-0.003320	0.000006
4	14	0	-0.203740	0.007894	0.000001

K-Si-Ca-F (s)

HF = -1666.943677 (a.u.)

Minimum vibrational frequencies ($\nu_{\min}/\text{cm}^{-1}$) = 34.1476

Standard orientation:

Center Number	Atomic Number	Atomic Type	Coordinates (Angstroms)		
			X	Y	Z
1	20	0	1.751447	0.001711	-0.341900
2	19	0	-2.909883	-0.778717	0.010173
3	9	0	3.367894	-0.884193	0.470720
4	14	0	-0.718015	1.622796	0.172017

K-Si-Ca-F (t)

HF = -1666.9662494 (a.u.)

Minimum vibrational frequencies ($\nu_{\min}/\text{cm}^{-1}$) = 24.0149

Standard orientation:

Center Number	Atomic Number	Atomic Type	Coordinates (Angstroms)		
			X	Y	Z
1	20	0	2.198906	-0.121323	-0.001429
2	19	0	-3.788880	0.062364	-0.001093
3	9	0	4.189128	0.243203	0.000417
4	14	0	-0.692254	-0.067663	0.003257

Li-Si-Be-Cl (s)

HF = -772.0299416 (a.u.)

Minimum vibrational frequencies ($\nu_{\min}/\text{cm}^{-1}$) = 85.1310

Standard orientation:

Center Number	Atomic Number	Atomic Type	Coordinates (Angstroms)		
			X	Y	Z
1	14	0	-2.010627	-0.423469	0.000003
2	4	0	0.138466	-0.145265	0.000000
3	3	0	-1.946061	2.099296	0.000000
4	17	0	1.966653	0.012455	-0.000002

Li-Si-Be-Cl (t)

HF = -772.0345305 (a.u.)

Minimum vibrational frequencies ($\nu_{\min}/\text{cm}^{-1}$) = 97.2869

Standard orientation:

Center Number	Atomic Number	Atomic Type	Coordinates (Angstroms)		
			X	Y	Z
1	14	0	-2.058309	-0.357639	-0.000013
2	4	0	0.110328	-0.102708	0.000021
3	3	0	-1.548272	1.984720	0.000048
4	17	0	1.942343	-0.031552	-0.000002

Li-Si-Mg-Cl (s)

HF = -957.3859687 (a.u.)

Minimum vibrational frequencies ($\nu_{\min}/\text{cm}^{-1}$) = 68.9228

Standard orientation:

Center Number	Atomic Number	Atomic Type	Coordinates (Angstroms)		
			X	Y	Z
1	12	0	-0.134676	-0.123912	-0.000039
2	3	0	2.592580	2.107991	0.000035
3	17	0	-2.372914	0.058493	0.000047
4	14	0	2.441279	-0.416529	-0.000031

Li-Si-Mg-Cl (t)

HF = -957.391269 (a.u.)

Minimum vibrational frequencies ($\nu_{\min}/\text{cm}^{-1}$) = 66.2104

Standard orientation:

Center Number	Atomic Number	Atomic Type	Coordinates (Angstroms)		
			X	Y	Z
1	12	0	0.115533	-0.006888	0.000121
2	3	0	-2.233914	1.990163	-0.000021
3	17	0	2.359063	-0.015588	-0.000082
4	14	0	-2.484909	-0.401631	0.000000

Li-Si-Ca-Cl (s)

HF = -1434.8856835 (a.u.)

Minimum vibrational frequencies ($\nu_{\min}/\text{cm}^{-1}$) = 22.7857

Standard orientation:

Center Number	Atomic Number	Atomic Type	Coordinates (Angstroms)		
			X	Y	Z
1	14	0	-2.738533	-0.364100	-0.242962
2	20	0	0.168729	-0.164788	0.353230
3	3	0	-2.975188	2.103822	0.062960
4	17	0	2.581791	0.122452	-0.226589

Li-Si-Ca-Cl (t)

HF = -1434.8934757 (a.u.)

Minimum vibrational frequencies ($\nu_{\min}/\text{cm}^{-1}$) = 19.5523

Standard orientation:

Center Number	Atomic Number	Atomic Type	Coordinates (Angstroms)		
			X	Y	Z
1	20	0	0.116400	0.047409	0.132250
2	3	0	-2.596574	2.056882	-0.099236
3	17	0	2.593586	-0.040994	-0.083053
4	14	0	-2.759230	-0.458710	-0.066814

Na-Si-Be-Cl (s)

HF = -926.8122095 (a.u.)

Minimum vibrational frequencies ($\nu_{\min}/\text{cm}^{-1}$) = 52.2079

Standard orientation:

Center Number	Atomic Number	Atomic Type	Coordinates (Angstroms)		
			X	Y	Z
1	14	0	1.336750	1.305842	0.000192
2	4	0	-0.645016	0.412711	-0.000034
3	11	0	2.169671	-1.412576	0.000123
4	17	0	-2.352989	-0.258488	-0.000229

Na-Si-Be-Cl (t)

HF = -926.8242844 (a.u.)

Minimum vibrational frequencies ($\nu_{\min}/\text{cm}^{-1}$) = 19.2194

Standard orientation:

Center Number	Atomic Number	Atomic Type	Coordinates (Angstroms)		
			X	Y	Z
1	14	0	-0.000109	0.005807	0.993232
2	4	0	0.000121	-0.006368	-1.101554
3	11	0	-0.000403	0.021195	3.666638
4	17	0	0.000323	-0.016998	-2.931297

Na-Si-Mg-Cl (s)

HF = -1112.1681373 (a.u.)

Minimum vibrational frequencies ($\nu_{\min}/\text{cm}^{-1}$) = 44.7962

Standard orientation:

Center Number	Atomic Number	Atomic Type	Coordinates (Angstroms)		
			X	Y	Z
1	14	0	1.818625	-1.235289	0.000022
2	12	0	-0.635467	-0.374065	0.000000
3	11	0	2.665396	1.487854	0.000002
4	17	0	-2.773794	0.318613	-0.000019

Na-Si-Mg-Cl (t)

HF = -1112.1706794 (a.u.)

Minimum vibrational frequencies ($\nu_{\min}/\text{cm}^{-1}$) = 49.3786

Standard orientation:

Center Number	Atomic Number	Atomic Type	Coordinates (Angstroms)		
			X	Y	Z
1	14	0	1.962837	-1.203405	0.000022
2	12	0	-0.506122	-0.302392	-0.000016
3	11	0	2.234337	1.594271	0.000012
4	17	0	-2.704939	0.172905	-0.000015

Na-Si-Ca-Cl (s)

HF = -1589.6666626 (a.u.)

Minimum vibrational frequencies ($\nu_{\min}/\text{cm}^{-1}$) = 15.2395

Standard orientation:

Center Number	Atomic Number	Atomic Type	Coordinates (Angstroms)		
			X	Y	Z
1	20	0	0.651072	-0.144706	0.326417
2	11	0	-3.225257	1.375049	-0.055097
3	17	0	3.052711	0.284643	-0.212891
4	14	0	-2.102835	-1.219311	-0.164509

Na-Si-Ca-Cl (t)

HF = -1589.6754919 (a.u.)

Minimum vibrational frequencies ($\nu_{\min}/\text{cm}^{-1}$) = 11.5414

Standard orientation:

Center Number	Atomic Number	Atomic Type	Coordinates (Angstroms)		
			X	Y	Z
1	20	0	0.496802	-0.152561	0.092853
2	11	0	-2.730780	1.570552	-0.019647
3	17	0	2.950766	0.209424	-0.058110
4	14	0	-2.147177	-1.270361	-0.046647

K-Si-Be-Cl (s)

HF = -1364.4491782 (a.u.)

Minimum vibrational frequencies ($\nu_{\min}/\text{cm}^{-1}$) = 34.8948

Standard orientation:

Center Number	Atomic Number	Atomic Type	Coordinates (Angstroms)		
			X	Y	Z
1	4	0	-1.200307	0.479589	0.000008
2	14	0	0.479018	1.839339	0.000022
3	19	0	2.289750	-0.890556	-0.000015
4	17	0	-2.671192	-0.632267	-0.000003

K-Si-Be-Cl (t)

HF = -1364.4679056 (a.u.)

Minimum vibrational frequencies ($\nu_{\min}/\text{cm}^{-1}$) = 26.4671

Standard orientation:

Center Number	Atomic Number	Atomic Type	Coordinates (Angstroms)		
			X	Y	Z
1	4	0	0.000000	0.000000	-1.784123
2	19	0	0.000000	0.000000	3.379051
3	17	0	0.000000	0.000000	-3.621579
4	14	0	0.000000	0.000000	0.321528

K-Si-Mg-Cl (s)

HF = -1549.8048658 (a.u.)

Minimum vibrational frequencies ($\nu_{\min}/\text{cm}^{-1}$) = 32.5639

Standard orientation:

Center Number	Atomic Number	Atomic Type	Coordinates (Angstroms)		
			X	Y	Z
1	14	0	1.063307	1.788440	0.000046
2	12	0	-1.169439	0.480769	0.000001
3	19	0	2.749383	-1.040447	0.000002
4	17	0	-3.123017	-0.649347	-0.000040

K-Si-Mg-Cl (t)

HF = -1549.82 39558 (a.u.)

Minimum vibrational frequencies ($\nu_{\min}/\text{cm}^{-1}$) = 20.7985

Standard orientation:

Center Number	Atomic Number	Atomic Type	Coordinates (Angstroms)		
			X	Y	Z
1	14	0	0.000000	0.000000	0.852405
2	12	0	0.000000	0.000000	-1.658493
3	19	0	0.000000	0.000000	3.916663
4	17	0	0.000000	0.000000	-3.908726

K-Si-Ca-Cl (s)

HF = -2027.3102916 (a.u.)

Minimum vibrational frequencies ($\nu_{\min}/\text{cm}^{-1}$) = 42.6300

Standard orientation:

Center Number	Atomic Number	Atomic Type	Coordinates (Angstroms)		
			X	Y	Z
1	14	0	2.498406	0.229852	0.000152
2	20	0	0.315096	-1.703942	-0.000113
3	19	0	-0.390928	2.109766	-0.000060
4	17	0	-1.991293	-0.542626	0.000074

K-Si-Ca-Cl (t)

HF = -2027.3253789 (a.u.)

Minimum vibrational frequencies ($\nu_{\min}/\text{cm}^{-1}$) = 20.0862

Standard orientation:

Center Number	Atomic Number	Atomic Type	Coordinates (Angstroms)		
			X	Y	Z
1	14	0	1.267772	0.102951	0.000229
2	20	0	-1.582795	0.227245	-0.000117
3	19	0	4.362734	-0.118288	-0.000063
4	17	0	-4.057932	-0.219925	0.000020

Li-Si-Be-Br (s)

HF = -2885.9461204 (a.u.)

Minimum vibrational frequencies ($\nu_{\min}/\text{cm}^{-1}$) = 79.5853

Standard orientation:

Center Number	Atomic Number	Atomic Type	Coordinates (Angstroms)		
			X	Y	Z
1	14	0	-2.747363	-0.414418	0.000003
2	4	0	-0.598960	-0.159044	0.000001
3	3	0	-2.607069	2.107361	0.000002
4	35	0	1.390861	0.003313	-0.000001

Li-Si-Be-Br (t)

HF = -2885.950687 (a.u.)

Minimum vibrational frequencies ($\nu_{\min}/\text{cm}^{-1}$) = 83.4106

Standard orientation:

Center Number	Atomic Number	Atomic Type	Coordinates (Angstroms)		
			X	Y	Z
1	14	0	2.783645	-0.353066	-0.000020
2	4	0	0.617984	-0.110898	0.000068
3	3	0	2.223009	1.986297	0.000050
4	35	0	-1.374628	-0.016354	-0.000004

Li-Si-Mg-Br (s)

HF = -3071.308062 (a.u.)

Minimum vibrational frequencies ($\nu_{\min}/\text{cm}^{-1}$) = 60.2667

Standard orientation:

Center Number	Atomic Number	Atomic Type	Coordinates (Angstroms)		
			X	Y	Z
1	12	0	-0.617243	-0.147302	0.000048
2	3	0	-3.312455	2.122803	-0.000021
3	35	0	1.775095	0.030368	-0.000036
4	14	0	-3.198860	-0.404548	0.000053

Li-Si-Mg-Br (t)

HF = -3071.313317 (a.u.)

Minimum vibrational frequencies ($\nu_{\min}/\text{cm}^{-1}$) = 58.8165

Standard orientation:

Center Number	Atomic Number	Atomic Type	Coordinates (Angstroms)		
			X	Y	Z
1	12	0	-0.631050	0.000047	0.000163
2	3	0	-2.989434	1.988273	0.000005
3	35	0	1.765434	-0.008283	-0.000067
4	14	0	-3.232092	-0.405391	0.000025

Li-Si-Ca-Br (s)

HF = -3548.8078185 (a.u.)

Minimum vibrational frequencies ($\nu_{\min}/\text{cm}^{-1}$) = 17.1636

Standard orientation:

Center Number	Atomic Number	Atomic Type	Coordinates (Angstroms)		
			X	Y	Z
1	14	0	-3.456610	-0.341213	-0.285198
2	20	0	-0.571387	-0.194018	0.397998
3	3	0	-3.671904	2.121498	0.071640
4	35	0	2.023885	0.065510	-0.119489

Li-Si-Ca-Br (t)

HF = -3548.8156207 (a.u.)

Minimum vibrational frequencies ($\nu_{\min}/\text{cm}^{-1}$) = 4.7249

Standard orientation:

Center Number	Atomic Number	Atomic Type	Coordinates (Angstroms)		
			X	Y	Z
1	14	0	3.487858	-0.429304	-0.013307
2	20	0	0.616825	-0.002006	0.023294
3	3	0	3.283312	2.087218	-0.012856
4	35	0	-2.029041	-0.006037	-0.006886

Na-Si-Be-Br (s)

HF = -3040.7283661 (a.u.)

Minimum vibrational frequencies ($\nu_{\min}/\text{cm}^{-1}$) = 45.9475

Standard orientation:

Center Number	Atomic Number	Atomic Type	Coordinates (Angstroms)		
			X	Y	Z
1	14	0	-2.167612	-1.285673	0.000267
2	4	0	-0.138687	-0.515129	0.000039
3	11	0	-2.789327	1.490836	0.000193
4	35	0	1.759541	0.104592	-0.000172

Na-Si-Be-Br (t)

HF = -3040.7402826 (a.u.)

Minimum vibrational frequencies ($\nu_{\min}/\text{cm}^{-1}$) = 17.7121

Standard orientation:

Center Number	Atomic Number	Atomic Type	Coordinates (Angstroms)		
			X	Y	Z
1	14	0	0.000000	0.000000	-1.904291
2	4	0	0.000000	0.000000	0.188644
3	11	0	0.000000	0.000000	-4.578759
4	35	0	0.000000	0.000000	2.179195

Na-Si-Mg-Cl (s)

HF = -3226.0902539 (a.u.)

Minimum vibrational frequencies ($\nu_{\min}/\text{cm}^{-1}$) = 13.9891

Standard orientation:

Center Number	Atomic Number	Atomic Type	Coordinates (Angstroms)		
			X	Y	Z
1	14	0	2.650667	-1.206519	0.000031
2	12	0	0.152374	-0.477455	0.000007
3	11	0	3.344213	1.561221	0.000007
4	35	0	-2.163547	0.155637	-0.000017

Na-Si-Mg-Br (t)

HF = -3226.0927981 (a.u.)

Minimum vibrational frequencies ($\nu_{\min}/\text{cm}^{-1}$) = 43.2760

Standard orientation:

Center Number	Atomic Number	Atomic Type	Coordinates (Angstroms)		
			X	Y	Z
1	14	0	2.748472	-1.182526	0.000031
2	12	0	0.254706	-0.345472	0.000000
3	11	0	2.941188	1.624103	0.000011
4	35	0	-2.111090	0.081026	-0.000016

Na-Si-Ca-Br (s)

HF = -3703.5888015 (a.u.)

Minimum vibrational frequencies ($\nu_{\min}/\text{cm}^{-1}$) = 13.9891

Standard orientation:

Center Number	Atomic Number	Atomic Type	Coordinates (Angstroms)		
			X	Y	Z
1	14	0	-2.913207	-1.133230	-0.298885
2	20	0	-0.111480	-0.411768	0.449022
3	11	0	-3.755050	1.551460	-0.005390
4	35	0	2.409144	0.200986	-0.135336

Na-Si-Ca-Br (t)

HF = -3703.5976371 (a.u.)

Minimum vibrational frequencies ($\nu_{\min}/\text{cm}^{-1}$) = 13.9498

Standard orientation:

Center Number	Atomic Number	Atomic Type	Coordinates (Angstroms)		
			X	Y	Z
1	14	0	-2.909044	-1.242038	-0.000113
2	20	0	-0.243333	-0.206474	0.000397
3	11	0	-3.432019	1.608058	-0.000121
4	35	0	2.381299	0.109411	-0.000144

K-Si-Be-Br (s)

HF = -3478.365586 (a.u.)

Minimum vibrational frequencies ($\nu_{\min}/\text{cm}^{-1}$) = 29.9098

Standard orientation:

Center Number	Atomic Number	Atomic Type	Coordinates (Angstroms)		
			X	Y	Z
1	4	0	-0.370787	0.751423	0.000011
2	14	0	1.453689	1.901208	0.000031
3	19	0	2.869544	-1.056495	-0.000013
4	35	0	-2.096852	-0.272834	-0.000007

K-Si-Be-Br (t)

HF = -3478.3839977 (a.u.)

Minimum vibrational frequencies ($\nu_{\min}/\text{cm}^{-1}$) = 23.1041

Standard orientation:

Center Number	Atomic Number	Atomic Type	Coordinates (Angstroms)		
			X	Y	Z
1	4	0	0.000000	0.000000	0.799945
2	19	0	0.000000	0.000000	-4.363946
3	35	0	0.000000	0.000000	2.798745
4	14	0	0.000000	0.000000	-1.302919

K-Si-Mg-Br (s)

HF = -3663.7270737 (a.u.)

Minimum vibrational frequencies ($\nu_{\min}/\text{cm}^{-1}$) = 27.6297

Standard orientation:

Center Number	Atomic Number	Atomic Type	Coordinates (Angstroms)		
			X	Y	Z
1	14	0	1.995290	1.800931	0.000066
2	12	0	-0.348320	0.701561	0.000011
3	19	0	3.412657	-1.173299	0.000012
4	35	0	-2.531277	-0.323974	-0.000036

K-Si-Mg-Br (t)

HF = -3663.7460724 (a.u.)

Minimum vibrational frequencies ($\nu_{\min}/\text{cm}^{-1}$) = 20.2012

Standard orientation:

Center Number	Atomic Number	Atomic Type	Coordinates (Angstroms)		
			X	Y	Z
1	14	0	0.000000	0.000000	-1.800172
2	12	0	0.000000	0.000000	0.712387
3	19	0	0.000000	0.000000	-4.865150
4	35	0	0.000000	0.000000	3.116903

K-Si-Ca-Br (s)

HF = -4141.2317487 (a.u.)

Minimum vibrational frequencies ($\nu_{\min}/\text{cm}^{-1}$) = 39.3180

Standard orientation:

Center Number	Atomic Number	Atomic Type	Coordinates (Angstroms)		
			X	Y	Z
1	20	0	-0.392073	-1.742749	0.000377
2	19	0	-0.653843	2.171805	0.000259
3	35	0	1.762818	-0.034209	-0.000186
4	14	0	-2.959583	-0.372285	-0.000426

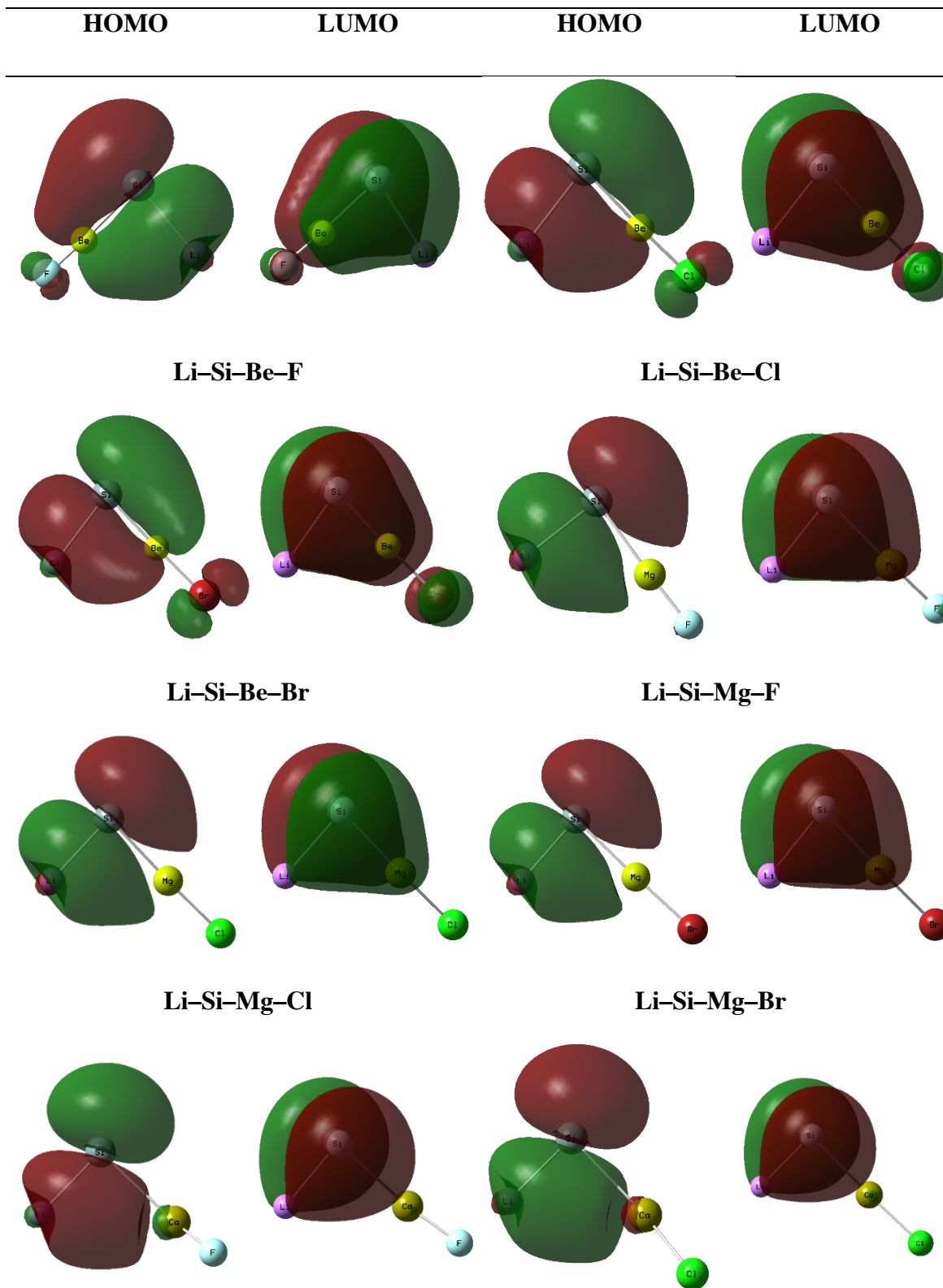
K-Si-Ca-Br (t)

HF = -4141.235557 (a.u.)

Minimum vibrational frequencies ($\nu_{\min}/\text{cm}^{-1}$) = 15.3970

Standard orientation:

Center Number	Atomic Number	Atomic Type	Coordinates (Angstroms)		
			X	Y	Z
1	14	0	-2.234888	1.765596	-0.000001
2	20	0	0.210222	0.065466	0.000085
3	19	0	-3.842478	-1.016159	0.000014
4	35	0	2.859745	-0.192018	-0.000056



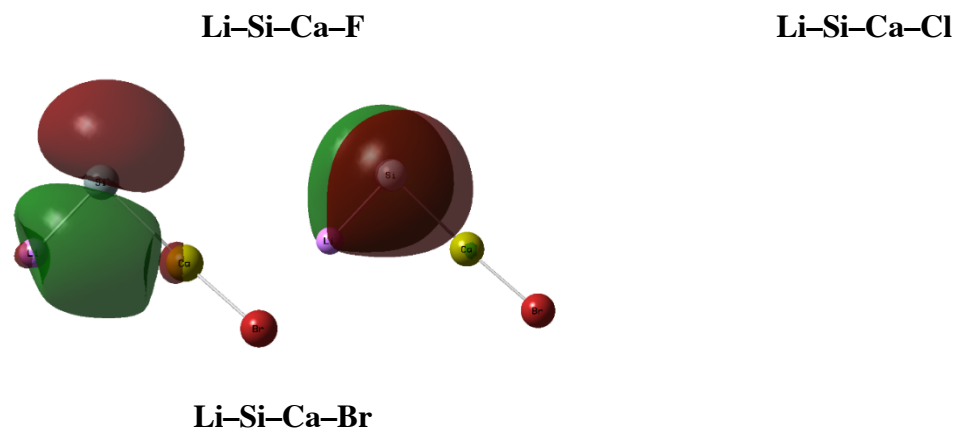
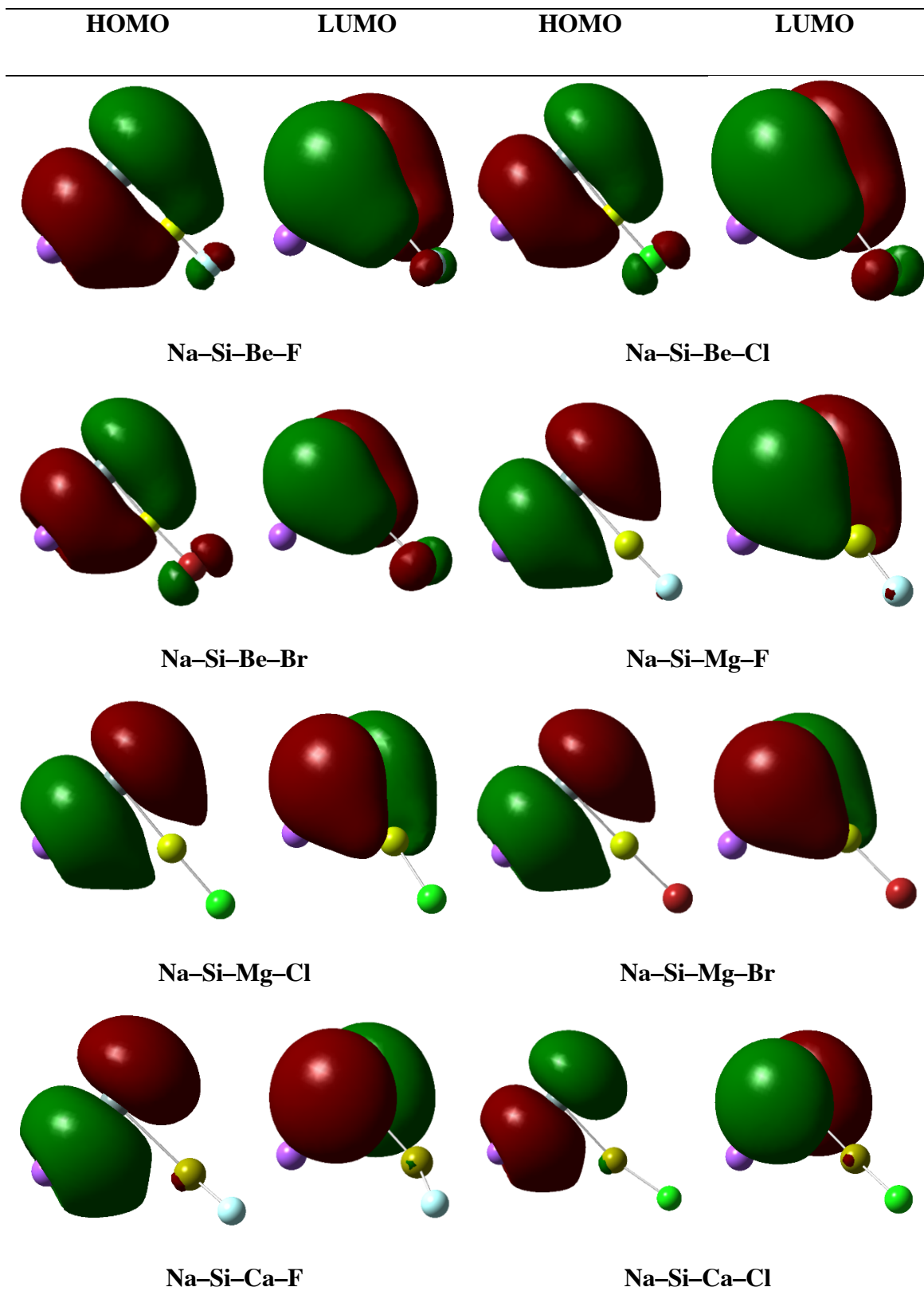
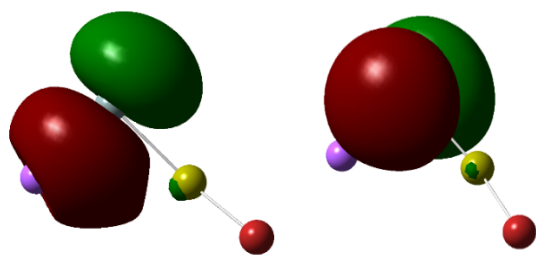


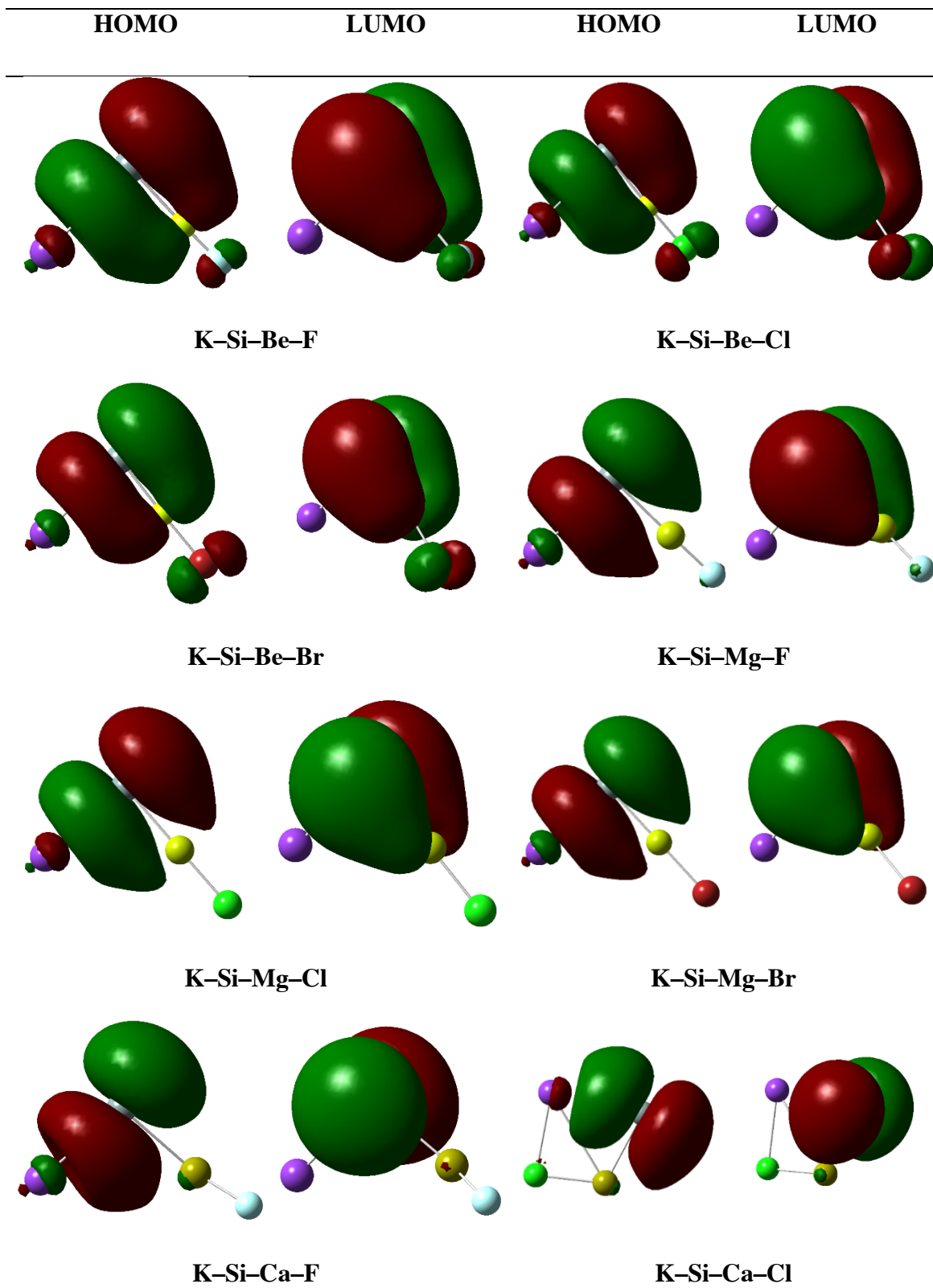
Figure S1. Shapes of selected molecular orbitals for singlet silylenes (Series 1).

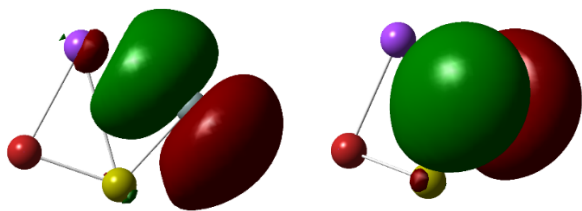




Na-Si-Ca-Br

Figure S2. Shapes of selected molecular orbitals for singlet silylenes (Series 2).





K-Si-Ca-Br

Figure S3. Shapes of selected molecular orbitals for singlet silylenes (Series 3).